

Article

Inter-Conversion between Different Compounds of Ternary Cs-Pb-Br System

Jing Li ^{1,2}, Huijie Zhang ¹, Song Wang ³, Debing Long ¹, Mingkai Li ¹, Duofa Wang ^{1,2,4,5,*}  and Tianjin Zhang ^{1,2,4,5,*}

¹ Department of Materials Science and Engineering, Hubei University, Wuhan 430062, China; lijing5781@hotmail.com (J.L.); huijie928@163.com (H.Z.); debinglong@foxmail.com (D.L.); mingkailee@hotmail.com (M.L.)

² Hubei Collaborative Innovation Center for Advanced Organic Chemical Materials, Hubei University, Wuhan 430062, China

³ Hubei Key Laboratory of Low Dimensional Optoelectronic Materials and Devices, Hubei University of Arts and Science, Xiangyang 441053, China; wangsong1984@126.com

⁴ Hubei Provincial Key Laboratory of Polymers, Hubei University, Wuhan 430062, China

⁵ Ministry of Education Key Laboratory of Green Preparation and Application for Materials, Hubei University, Wuhan 430062, China

* Correspondence: duofawang@hotmail.com (D.W.); zhangtj@hubu.edu.cn (T.Z.); Tel.: +86-27-8866-1729 (D.W. & T.Z.)

Received: 1 April 2018; Accepted: 1 May 2018; Published: 2 May 2018



Abstract: The perovskite CsPbBr₃ attracts great attention due to its potential in optoelectronics. However, stability remains a major obstacle to achieving its effecting application. In this work, we prepared CsPbBr₃ solids through a simple reaction and investigated reversible conversion between CsPbBr₃, Cs₄PbBr₆, and CsPb₂Br₅. We found that CsPbBr₃ can be respectively converted to Cs₄PbBr₆ or CsPb₂Br₅ by reacting with CsBr or PbBr₂. Thermodynamic analysis demonstrated that the chemical reactions above were exothermic and occurred spontaneously. Moreover, the formed Cs₄PbBr₆ could be converted to CsPbBr₃ reversely, and then progressively converted to Cs-deficient CsPb₂Br₅ by extraction of CsBr with water. The CsPb₂Br₅ was converted to CsPbBr₃ reversely under thermal annealing at 400 °C. The thermodynamic processes of these conversions between the three compounds above were clarified. Our findings regarding the conversions not only provide a new method for controlled synthesis of the ternary Cs-Pb-Br materials but also clarify the underlying mechanism for the instability of perovskites CsPbBr₃.

Keywords: CsPbBr₃; Cs₄PbBr₆; CsPb₂Br₅; perovskite; conversion

1. Introduction

All-inorganic cesium lead halide perovskite CsPbX₃ (X = I, Br, Cl) nanocrystals (NCs) have attracted considerable attention owing to the outstanding photophysical properties, such as high photoluminescence quantum yields, narrow emission bandwidths, and tunable band gaps that covers the full visible range [1,2]. Since the pioneering work by the Kovalenko group in 2015, considerable progress in the preparation and application of CsPbBr₃ NCs has been achieved within a very short time period [1]. CsPbBr₃ NCs with a controllable morphology and composition have been fabricated by different methods, such as hot-injection [3], solvothermal synthesis [4], room-temperature precipitation [5], and chemical vapor deposition (CVD) [6]. Moreover, a variety of photoelectronic devices—such as photovoltaics [7], lasing [8], light-emitting diodes and photodetectors [9,10]—have been prepared from CsPbBr₃ NC. In addition to CsPbBr₃ NCs, other types of materials of the ternary Cs-Pb-Br system, such as Cs₄PbBr₆ and CsPb₂Br₅, have also been reported [11,12]. The compounds

CsPbBr₃, Cs₄PbBr₆, and CsPb₂Br₅ differ in the stacking of PbBr₆ octahedra in their crystal structures. In CsPbBr₃, the lead halide octahedra share all corners and are electronically coupled in three directions in space. However, in the Cs₄PbBr₆ lattice the octahedra do not share any corners [11]. One lead atom and eight bromine atoms make up a hendecahedron with edge sharing in CsPb₂Br₅ [12]. It is reasonable to suspect that the existence of multiple compounds of Cs-Pb-Br system is probably relevant to the unstable luminescent property of CsPbBr₃, which is the main obstacle on the progress of CsPbBr₃. The photoluminescence quantum yield (PLQY) of colloidal CsPbBr₃ NCs of ~90% decreases dramatically to below ~20% when they are in the solid phase (such as in a thin film). Different mechanisms have been proposed to explain the luminescence quenching, such as loss of the high quality of the NC by aggregation, removal of the surface passivation, and chemical decomposition of the materials [11,13]. Therefore, investigation on the inter-conversion between the Cs-Pb-Br compounds above is rather important.

Very recently, it has been reported that these ternary Cs-Pb-Br compounds can be inter-converted by physical and chemical treatments. Conversion of pre-synthesized CsPbBr₃ NC to Cs₄PbBr₆ NCs have been reported by the extraction of PbBr₂ through amine- and thiol-mediation method [14,15]. Furthermore, a reverse conversion from Cs₄PbBr₆ to CsPbBr₃ has been reported by the Manna group through extraction of CsBr with Prussian Blue [16]. However, all the conversions above were performed on Cs-Pb-Br NCs with ligands on their surface and they were realized with mediation by a ligand. Investigations on the inter-conversion between the bare compounds of the Cs-Pb-Br system without ligand mediation are rarely reported, which is essential to reveal instability mechanism of CsPbBr₃.

In this work, we prepared CsPbBr₃ particles without ligands through a simple low temperature method and realized reversible conversions between CsPbBr₃ and Cs₄PbBr₆, and between CsPbBr₃ and CsPb₂Br₅. We combined our experimental observations with calculations of the total energy of the three Cs-Pb-Br compounds, we found that conversions of CsPbBr₃ to Cs₄PbBr₆ and to CsPb₂Br₅ could take place spontaneously. However, the reverse conversions required external intervention.

2. Materials and Methods

2.1. Materials

Lead(II) bromide (PbBr₂, Aladdin, 99.999%), cesium bromide (CsBr, Aladdin, 99.999%), hydrobromic acid (HBr, ≥40.0%), and *N,N*-dimethylformamide (DMF, Aladdin, 99.9%), were used without any further purification.

2.2. Synthesis of CsPbBr₃

The synthesis of CsPbBr₃ was performed via a simple reaction and crystallization method. Briefly, 0.5 mmol of PbBr₂ and 0.5 mmol of CsBr were dissolved in 10 mL of DMF and stirred until completely dissolved. The mixture was then placed in an oven at 40 °C to evaporate the solvent and induce the reaction to produce CsPbBr₃ solids.

2.3. Experiments on the Inter-Conversion between the Compounds

2.3.1. Forward Conversion from CsPbBr₃ to Cs₄PbBr₆ or CsPb₂Br₅

Cesium bromide (CsBr, 3 mmol) was first dissolved in hydrobromic acid (HBr, 2 mL). Pre-synthesized CsPbBr₃ (1 mmol) was added to the solution and stirred to react with CsBr and produce Cs₄PbBr₆, which precipitated at the bottom of the mixture. The precipitate was collected by evaporating the HBr solvent. For the conversion to CsPb₂Br₅, lead(II) bromide (PbBr₂, 1 mmol) was first dissolved in hydrobromic acid (HBr, 2 mL). Then the CsPbBr₃ solid (1 mmol) was added to the solution with stirring to react with PbBr₂. The CsPb₂Br₅ was produced and precipitated at the bottom of the mixture. The precipitate was collected by evaporating the HBr solvent.

2.3.2. Reverse Conversion from Cs₄PbBr₆ or CsPb₂Br₅ to CsPbBr₃

A 0.25 mmol portion of Cs₄PbBr₆ was added to de-ionized water (1 mL) and stirred, to trigger the reverse conversion from Cs₄PbBr₆ to CsPbBr₃. The conversion of CsPb₂Br₅ to CsPbBr₃ was conducted by annealing the CsPb₂Br₅ solids for 4 h at 400 °C in air.

2.4. Materials Characterization

Crystal structures were measured with an X-ray diffractometer (Bruker D8 Advance, Karlsruhe, Baden-Wuerttemberg, Germany) with Cu-Kα radiation ($\lambda = 1.5406 \text{ \AA}$). Scanning electron microscope (SEM) and energy dispersive spectrum (EDS) measurements were performed on a JSM7100F, Tokyo, Honshu, Japan. A transmission electron microscope (TEM) (FEI; Tecnai-G20 and 200 kV, Hillsboro, OR, USA) was used to characterize the microstructure of the CsPbBr₃, Cs₄PbBr₆ and CsPb₂Br₅. Absorption spectra were measured on a UV-Visible-NIR spectrophotometer (SHIMADZU UV-3600, Kyoto, Honshu, Japan).

2.5. First-Principle Calculations

First-principle calculations were performed on the basis of density functional theory (DFT) as implemented in the QUANTUM ESPRESSO (QE) code. The exchange and correlation terms were described using the general gradient approximation (GGA) of Perdew-Burke-Ernzerhof (PBE). The energy cutoff for the plane wave basis set was 600 eV. The accuracy of the self-consistent field (SCF) energy convergence and the convergence accuracy of the internal stress of the crystal were less than 1.4×10^{-5} eV/atom and 0.05 Gpa, respectively. For the different alloy configurations, Monkhorst-Pack grids were determined automatically for the Brillouin zone integration and the KPPRA parameter was set to be 1000.

3. Results and Discussion

3.1. Synthesis of CsPbBr₃ and Forward Conversion to Cs₄PbBr₆ and CsPb₂Br₅.

Synthesis of CsPbBr₃ (PDF#18-0364) was performed via a simple reaction and crystallization method without the use of any ligands. Full details are described in the experimental section. Characterization results of the prepared solids by XRD and absorption spectroscopy, shown in Figure 1a,b, demonstrated that the product was pure monoclinic CsPbBr₃.

The as-synthesized CsPbBr₃ solids were used to perform the forward conversion from CsPbBr₃ to Cs₄PbBr₆ and CsPb₂Br₅. First, CsBr was dissolved in HBr, and a certain amount of the CsPbBr₃ solid synthesized above (yellow) was added into the solution (CsPbBr₃/CsBr = 1:3, mole ratio) with stirring. This approach ensured that only H was introduced into the reaction system, containing Cs, Pb, and Br, which simplified the analysis on the reaction. After stirring for several hours, a white precipitate formed, which was revealed to be rhombohedral Cs₄PbBr₆ by XRD, as shown in Figure 1c. To reveal whether CsPbBr₃ remnants exist in the product since both CsPbBr₃ and Cs₄PbBr₆ exhibit diffraction peaks near 27°, the absorption spectrum of Cs₄PbBr₆ product was measured and is shown in Figure 1d. A typical absorption peak at 315 nm was observed, which is characteristic of Cs₄PbBr₆, and no absorption peaks corresponding to CsPbBr₃ appear [17]. This result further confirmed the conversion from CsPbBr₃ to Cs₄PbBr₆. As far as the additional small diffraction peak near 29° denoted by purple dot in Figure 1c is concerned, it corresponds to CsBr. Because the ratio of the reactants CsPbBr₃/CsBr was 1:3 and the only product was Cs₄PbBr₆, Equation (1) is proposed to describe the chemical reaction of the conversion. Except for operating as the solvent, the HBr also supplies abundance of Br⁺ and promotes the chemical reaction according to Equation (1).



The conversion from CsPbBr_3 to CsPb_2Br_5 was realized by a similar reaction. First, PbBr_2 was dissolved in HBr and CsPbBr_3 solid was added into the solution ($\text{CsPbBr}_3/\text{PbBr}_2 = 1:1$, mole ratio). After several hours, white solids precipitated at the bottom of the mixture. XRD characterization, as shown in Figure 1e, of the precipitate revealed that it was pure tetragonal CsPb_2Br_5 , indicating that the conversion from CsPbBr_3 to CsPb_2Br_5 occurred. To confirm the conversion, the absorption spectra of the reactant and product were measured. As shown in Figure 1f, the absorption edge moved to 380 nm, indicating that CsPbBr_3 was converted into CsPb_2Br_5 . The conversion was believed to occur through Equation (2), as shown below, based on the fact that the ratio of the reactants $\text{CsPbBr}_3/\text{PbBr}_2$ was 1:1 and the only product formed was CsPb_2Br_5 .

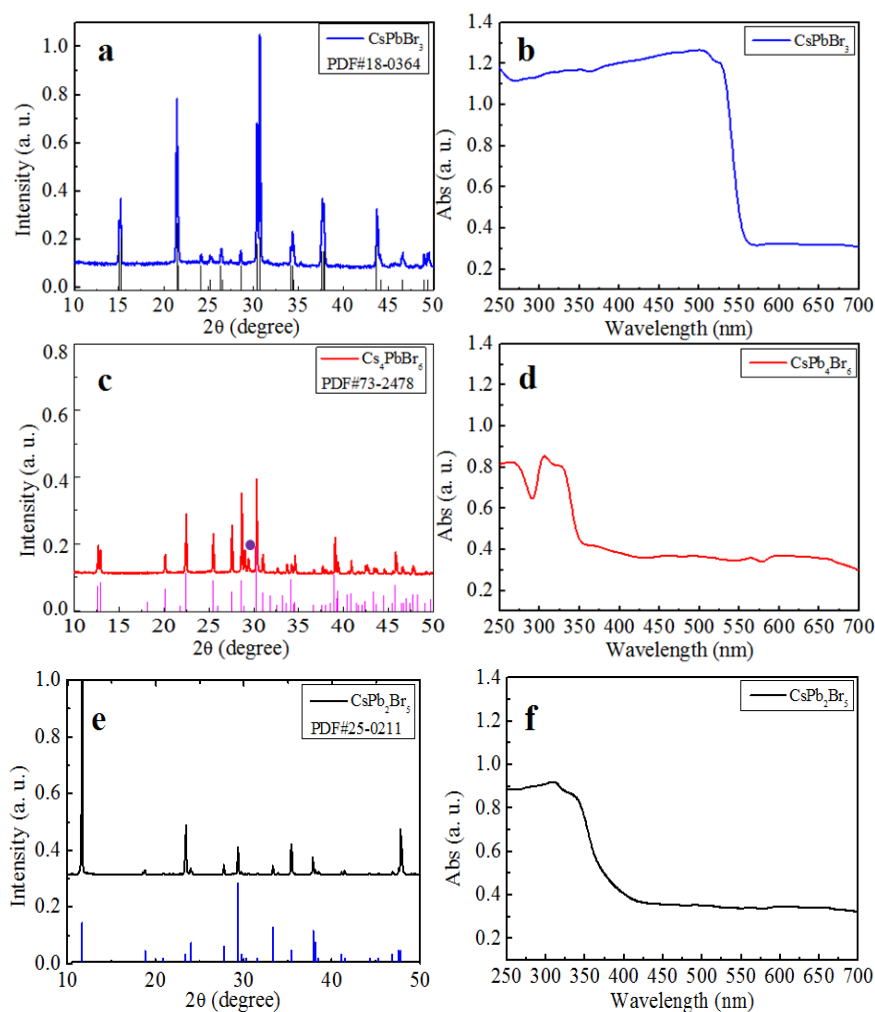
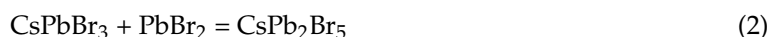


Figure 1. The XRD pattern of (a) CsPbBr_3 , (c) Cs_4PbBr_6 and (e) CsPb_2Br_5 . The absorption spectra of (b) CsPbBr_3 , (d) Cs_4PbBr_6 , and (f) CsPb_2Br_5 .

The morphology of each material was examined by scanning electron microscope (SEM) imaging, as shown in Figure S1. Energy dispersive spectroscopy (EDS) results, also shown in Figure S1, indicated that the molar ratios of $\text{Cs}/\text{Pb}/\text{Br}$ were 1.18/1/2.89, 1/1.87/5.57, and 4.18/1/6.36 respectively, which agreed well with the stoichiometries of CsPbBr_3 , CsPb_2Br_5 , and Cs_4PbBr_6 . The microstructure of each Cs-Pb-Br ternary compound was characterized by high resolution TEM (HRTEM), as shown in Figure 2. Well-resolved lattice fringes were observed in the HRTEM images. In Figure 2b, the separation between

the fringes was 0.588 nm, which corresponded to the (001) plane of CsPbBr₃. In the HRTEM images of CsPb₂Br₅ and Cs₄PbBr₆, the (110) and (220) planes were clearly observed, with lattice separations of 0.609 and 0.451 nm, respectively. These EDS and HRTEM results further confirmed that the conversions had occurred.

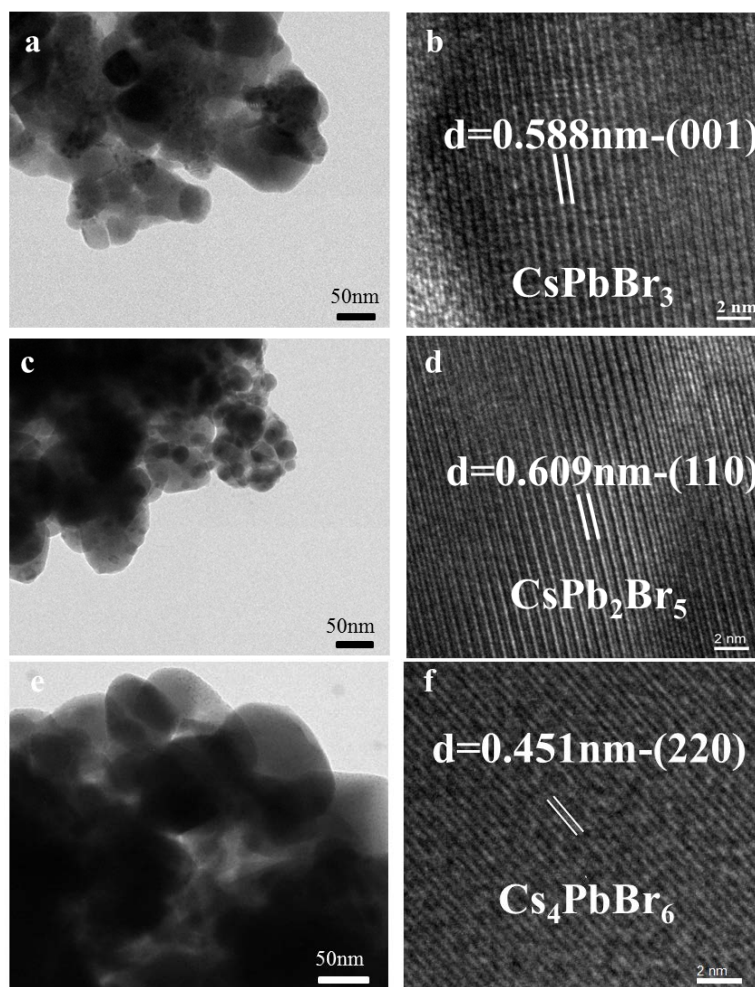


Figure 2. (a,c,e) TEM images; and (b,d,f) high-resolution lattice resolved TEM images of a representative CsPbBr₃, CsPb₂Br₅, and Cs₄PbBr₆, respectively.

In the conversions above, we did not use high temperature, high pressure or a catalyst to trigger the reactions. Hence, the Equations (1) and (2) are thermodynamically controlled process and the driving force, described by the free energy should be negative. Therefore, we calculated the total energy (E_t) of the Equations (1) and (2) by first principles. The changes of the total energy (ΔE_t) for Equations (1) and (2) were -9508.07 eV and -15019.13 eV, respectively, indicating that the chemical reactions were exothermic and could occur spontaneously. The total energy of each materials is shown in Table S1 in the supporting information. These results explain why this simple method can successfully realize the conversion of CsPbBr₃ into Cs₄PbBr₆ or CsPb₂Br₅.

3.2. Reverse Conversion by Water Extraction and Thermal Annealing

For the reverse conversion from Cs₄PbBr₆ to CsPbBr₃, we used the water extraction method proposed by the Sun group [18]. By mixing a Cs₄PbBr₆ quantum dot dispersion in nonpolar hexane with water, Sun et al. found that CsBr could be extracted from Cs₄PbBr₆ owing to the high solubility of CsBr in water. This effect led to a conversion from Cs₄PbBr₆ to CsPbBr₃.

Here, we found that water could also extract CsBr from Cs₄PbBr₆ solids without ligands on their surface. However, the reaction we observed was much more vigorous and quick. These differences between our observations and those of Sun et al. could be attributed to the absence of protective ligands on the surface of our NCs, unlike the Cs₄PbBr₆ quantum dot dispersion reported by Sun [18]. When the Cs₄PbBr₆ solids were added into deionized water, the color of the precipitate changed to yellow immediately, and returned to white again over a longer time, suggesting that chemical reactions occurred in two stages. The precipitate at different stages was removed from the deionized water and the composition was measured by XRD.

As shown in Figure 3a, most of the Cs₄PbBr₆ transformed to CsPbBr₃ within 1 min. However, CsPbBr₃ was not the final product. The conversion into CsPb₂Br₅ proceeded within 5 min, and the major product was CsPb₂Br₅ after 1 h. Therefore, we suggest that the water not only extracted CsBr from Cs₄PbBr₆, but also extracted CsBr from CsPbBr₃ to produce CsPb₂Br₅. The composition of the solution was also investigated to clarify the nature of the chemical transformation. To confirm the water extraction mechanism for the conversions, we evaporated the water and performed XRD measurements on the solid obtained, which was determined to be CsBr, as shown in the supporting information Figure S2. Therefore, we propose the following Equations for the chemical reactions occurring at each stage of the transformation as:



Figure 3b shows the absorption spectrum measured from the precipitate samples removed from deionized water after different reaction times. A strong characteristic absorption edge at 560 nm appeared after 1 min and its intensity decreased at longer reaction times. This result indicates that the CsPbBr₃ was produced within 1 min and converted to CsPb₂Br₅ over longer reaction times. These findings are consistent with the XRD results.

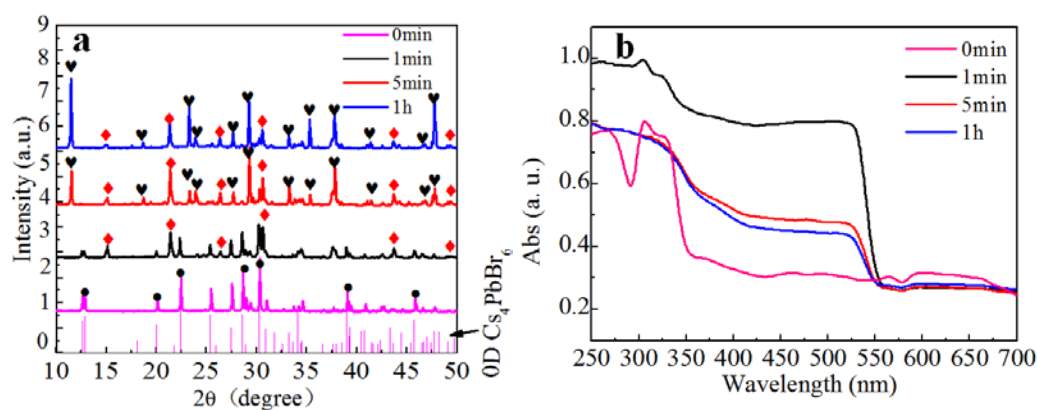


Figure 3. (a) PXRD pattern of Cs₄PbBr₆ solids after water treatment for different time, the red diamonds represent CsPbBr₃, the black hearts represents CsPb₂Br₅, the black dots represents Cs₄PbBr₆; (b) Absorption spectra of PXRD pattern of Cs₄PbBr₆ solids after water treatment for different times.

To confirm the two-step transformation model suggested above, we added pure CsPbBr₃ into deionized water and investigated the conversion. We found that the transformation in Equation (4) occurred and a white precipitate was formed quickly. As shown in the XRD pattern obtained from the precipitate in Figure 4a, the diffraction peaks related to CsPbBr₃ became weak and strong diffraction peaks corresponding to CsPb₂Br₅ were observed after 1 min. Moreover, the intensity of CsPb₂Br₅ gradually increased as the reaction progressed. The absorption spectra in Figure 4b, show that the absorption peak at 560 nm from CsPbBr₃ became progressively weaker. We note that the absorption

peak of CsPbBr_3 did not completely disappear, even after 1 h of reaction, indicating that a small amount of CsPbBr_3 persisted. The XRD and absorption results clearly demonstrated that CsPbBr_3 could be converted to CsPb_2Br_5 through extraction of CsBr by water. The conversion induced by water extraction is undoubtedly one of the reasons leading to the unstable luminescent property of CsPbBr_3 . The water vapor in the air can extract CsBr from CsPbBr_3 and trigger the conversion into CsPb_2Br_5 , which subsequently results in the degradation of luminescence.

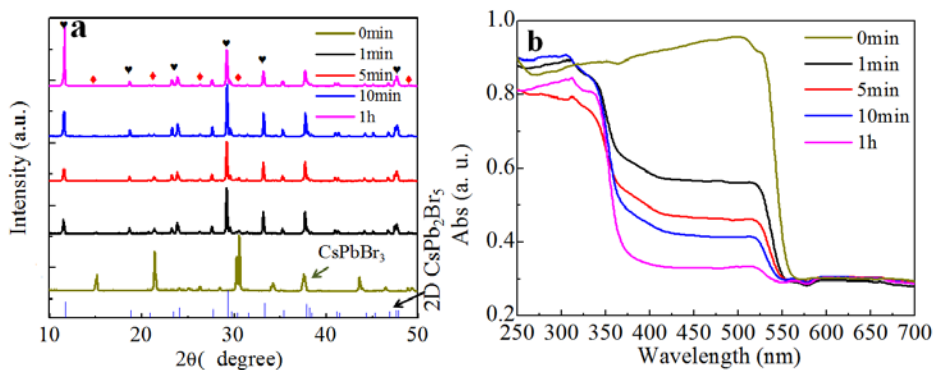


Figure 4. (a) XRD patterns and (b) absorption spectra of CsPbBr_3 solids after water treatment for different times. Red diamonds represent CsPbBr_3 and black hearts denote the diffraction peaks of CsPb_2Br_5 .

We realized a conversion from CsPb_2Br_5 to CsPbBr_3 , using a previously reported annealing method [19]. We annealed the CsPb_2Br_5 solids at $400\text{ }^\circ\text{C}$ in air for 4 h and monitored the associated XRD and absorption properties. Figure 5a shows XRD data of the CsPb_2Br_5 before and after annealing. The corresponding diffraction peaks before annealing were indexed to CsPb_2Br_5 . After annealing, the main product corresponded to CsPbBr_3 and PbBr_2 , and a small amount of CsPb_2Br_5 remained. The decomposition is depicted by the Equation:



The absorption spectra in Figure 5b show that the absorption peak relevant to CsPbBr_3 was considerably enhanced, indicating the generation of CsPbBr_3 , which is consistent with the XRD results shown in Figure 5a. As far as the mechanism of the Equation (5) is concerned, it is ascribed to the decomposition of CsPb_2Br_5 energetically driven by high temperature annealing.

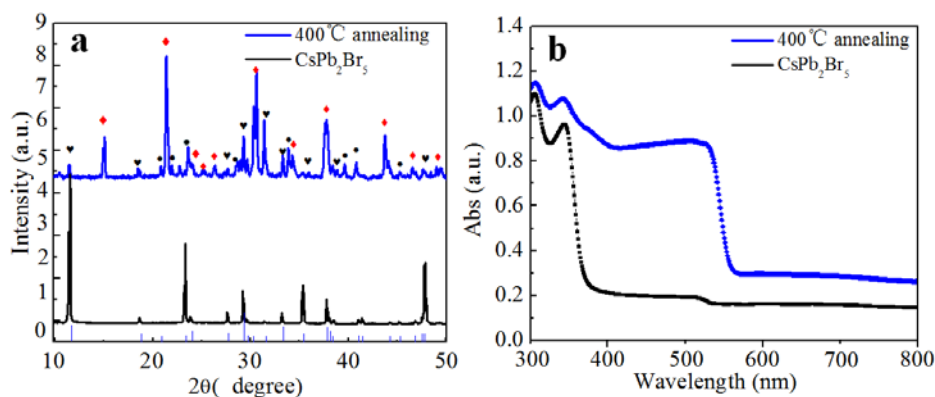


Figure 5. (a) XRD pattern, and (b) absorption spectra of CsPb_2Br_5 particles after annealing at $400\text{ }^\circ\text{C}$ temperature. In the XRD pattern, the red diamonds denotes the diffraction peak of CsPbBr_3 , the black dots denotes the diffraction peak of PbBr_2 and black hearts denote the diffraction peaks of CsPb_2Br_5 .

4. Conclusions

In conclusion, we examined a reversible conversion between CsPbBr₃, Cs₄PbBr₆, and CsPb₂Br₅. First, CsPbBr₃ solids were synthesized through a simple reaction of CsBr and PbBr₂ in HBr. Addition of the prepared CsPbBr₃ solids into the CsBr/PbBr₂ solution in HBr, resulted in its conversion into Cs₄PbBr₆ and CsPb₂Br₅, through Equations (1) and (2), respectively. Thermodynamic analysis revealed that the transformations above were exothermic and occurred spontaneously. Moreover, we found that when added into the water Cs₄PbBr₆ converted to CsPbBr₃ first, and then to Cs-deficient CsPb₂Br₅. These results are attributed to the ionic nature of the Cs-Pb-Br system and the high solubility of CsBr in water, which led to extraction of CsBr by water. The CsPb₂Br₅ was converted to CsPbBr₃ through thermal annealing at 400 °C. Our results on the inter-conversion of the Cs-Pb-Br compounds sheds a light on understanding the mechanism and developing new solutions for the instability problem of the Cs-Pb-Br compounds. Moreover, it supplies important information on the controllable preparation of the Cs-Pb-Br materials.

Supplementary Materials: The following are available online at <http://www.mdpi.com/1996-1944/11/5/717/s1>, Figure S1: Scanning electron microscope (SEM) and Energy dispersive X-spectroscopy (EDS); Figure S2: The XRD pattern of CsBr (PDF#73-0391) obtained from the solvent of water by evaporation; Table S1. The total energy of each materials is calculated based on the optimized structure using DFT.

Author Contributions: J.L., H.Z., and S.W. performed the experiments; D.L. and M.L. performed the calculation; D.W. and T.Z. design this study and analyzed the data; all authors read and approved the final manuscript.

Funding: This research was funded by National Natural Science Foundation of China (nos. 11174071, 11304088 and 51372180) and Special Technical Innovation Project of Hubei Province (no. 2016AAA035).

Acknowledgments: We thank Zhijun Ma in Hubei University for his help on the XRD measurement and analysis.

Conflicts of Interest: The authors declare no conflicts of interest.

References

1. Zhang, J.; Yang, Y.; Deng, H.; Farooq, U.; Yang, X.K.; Kan, J.; Tang, J.; Song, H.S. High quantum yield blue emission from lead-free inorganic antimony halide perovskite colloidal quantum dot. *ACS Nano* **2017**, *11*, 9294–9302. [[CrossRef](#)] [[PubMed](#)]
2. Protesescu, L.; Yakunin, S.; Bodnarchuk, M.I.; Krieg, F.; Caputo, R.; Hendon, C.H.; Yang, R.X.; Walsh, A.; Kovalenko, M.V. Nanocrystals of cesium lead halide perovskites (CsPbX₃, X = Cl, Br, and I): novel optoelectronic materials showing bright emission with wide color gamut. *Nano Lett.* **2015**, *15*, 3692–3696. [[CrossRef](#)] [[PubMed](#)]
3. Pan, A.; He, B.; Fan, X.; Liu, Z.; Urban, J.J.; Alivisatos, A.P.; He, L.; Liu, Y. Insight into the ligand-mediated synthesis of colloidal CsPbBr₃ perovskite nanocrystals: the role of organic acid, base, and cesium precursors. *ACS Nano* **2016**, *10*, 7943–7954. [[CrossRef](#)] [[PubMed](#)]
4. Rakita, Y.; Kedem, N.; Gupta, S.; Sadhanala, A.; Kalchenko, V.; Böhm, M.L.; Kulbak, M.; Friend, R.H.; Cahen, D.; Hodes, G. Low-temperature solution-grown CsPbBr₃ single crystals and their characterization. *Cryst. Growth Des.* **2016**, *16*, 5717–5725. [[CrossRef](#)]
5. Sun, S.; Yuan, D.; Xu, Y.; Wang, A.; Deng, Z. Ligand-mediated synthesis of shape-controlled cesium lead halide perovskite nanocrystals via reprecipitation process at room temperature. *ACS Nano* **2016**, *10*, 3648–3657. [[CrossRef](#)] [[PubMed](#)]
6. Wang, Y.; Guan, X.; Li, D.; Cheng, H.-C.; Duan, X.; Lin, Z.; Duan, X. Chemical vapor deposition growth of single-crystalline cesium lead halide microplatelets and heterostructures for optoelectronic applications. *Nano Res.* **2017**, *10*, 1223–1233. [[CrossRef](#)]
7. Swarnkar, A.; Marshall, A.R.; Sanehira, E.M.; Chernomordik, B.D.; Moore, D.T.; Christians, J.A.; Chakrabarti, T.; Luther, J.M. Quantum dot-induced phase stabilization of α -CsPbI₃ perovskite for high-efficiency photovoltaics. *Science* **2016**, *354*, 92–95. [[CrossRef](#)] [[PubMed](#)]
8. Eaton, S.W.; Lai, M.; Gibson, N.A.; Wong, A.B.; Dou, L.; Ma, J.; Wang, L.-W.; Leone, S.R.; Yang, P. Lasing in robust cesium lead halide perovskite nanowires. *Proc. Natl. Acad. Sci. USA* **2016**, *113*, 1993–1998. [[CrossRef](#)] [[PubMed](#)]

9. Song, J.; Li, J.; Li, X.; Xu, L.; Dong, Y.; Zeng, H. Quantum dot light-emitting diodes based on inorganic perovskite cesium lead halides (CsPbX_3). *Adv. Mater.* **2015**, *27*, 7162–7167. [[CrossRef](#)] [[PubMed](#)]
10. Ramasamy, P.; Lim, D.-H.; Kim, B.; Lee, S.-H.; Lee, M.-S.; Lee, J.-S. All-inorganic cesium lead halide perovskite nanocrystals for photodetector applications. *Chem. Commun.* **2016**, *52*, 2067–2070. [[CrossRef](#)] [[PubMed](#)]
11. Saidaminov, M.I.; Almutlaq, J.; Sarmah, S.; Dursun, I.; Zhumekenov, A.A.; Begum, R.; Pan, J.; Cho, N.; Mohammed, O.F.; Bakr, O.M. Pure Cs_4PbBr_6 : Highly luminescent zero-dimensional perovskite solids. *ACS Energy Lett.* **2016**, *1*, 840–845. [[CrossRef](#)]
12. Wang, K.H.; Wu, L.; Li, L.; Yao, H.B.; Qian, H.S.; Yu, S.H. Large-scale synthesis of highly luminescent perovskite-related CsPb_2Br_5 nanoplatelets and their fast anion exchange. *Angew. Chem. Int. Ed.* **2016**, *55*, 8328–8332. [[CrossRef](#)] [[PubMed](#)]
13. Zhang, Y.; Saidaminov, M.I.; Dursun, I.; Yang, H.; Murali, B.; Alarousu, E.; Yengel, E.; Alshankiti, B.A.; Bakr, O.M.; Mohammed, O.F. Zero-dimensional Cs_4PbBr_6 perovskite nanocrystals. *J Phys. Chem. Lett.* **2017**, *8*, 961–965. [[CrossRef](#)] [[PubMed](#)]
14. Liu, Z.; Bekenstein, Y.; Ye, X.; Nguyen, S.C.; Swabeck, J.; Zhang, D.; Lee, S.-T.; Yang, P.; Ma, W.; Alivisatos, A.P. Ligand mediated transformation of cesium lead bromide perovskite nanocrystals to lead depleted Cs_4PbBr_6 nanocrystals. *J Am. Chem. Soc.* **2017**, *139*, 5309–5312. [[CrossRef](#)] [[PubMed](#)]
15. Palazon, F.; Almeida, G.; Akkerman, Q.A.; De Trizio, L.; Dang, Z.; Prato, M.; Manna, L. Changing the dimensionality of cesium lead bromide nanocrystals by reversible postsynthesis transformations with Amines. *Chem. Mater.* **2017**, *29*, 4167–4171. [[CrossRef](#)] [[PubMed](#)]
16. Palazon, F.; Urso, C.; De Trizio, L.; Akkerman, Q.; Marras, S.; Locardi, F.; Nelli, I.; Ferretti, M.; Prato, M.; Manna, L. Postsynthesis Transformation of insulating Cs_4PbBr_6 nanocrystals into bright perovskite CsPbBr_3 through physical and chemical extraction of CsBr. *ACS Energy Lett.* **2017**, *2*, 2445–2448. [[CrossRef](#)] [[PubMed](#)]
17. Quan, L.N.; Quintero-Bermudez, R.; Voznyy, O.; Walters, G.; Jain, A.; Fan, J.Z.; Zheng, X.; Yang, Z.; Sargent, E.H. Highly emissive green perovskite nanocrystals in a solid state crystalline matrix. *Adv. Mater.* **2017**, *29*, 1605945. [[CrossRef](#)] [[PubMed](#)]
18. Wu, L.; Hu, H.; Xu, Y.; Jiang, S.; Chen, M.; Zhong, Q.; Yang, D.; Liu, Q.; Zhao, Y.; Sun, B. From nonluminescent Cs_4PbX_6 ($X = \text{Cl}, \text{Br}, \text{I}$) nanocrystals to highly luminescent CsPbX_3 nanocrystals: water-triggered transformation through a CsX-stripping mechanism. *Nano Lett.* **2017**, *17*, 5799–5804. [[CrossRef](#)] [[PubMed](#)]
19. Li, J.; Zhang, H.; Wang, S.; Long, D.; Li, M.; Guo, Y.; Zhong, Z.; Wu, K.; Wang, D.; Zhang, T. Synthesis of all-inorganic CsPb_2Br_5 perovskite and determination of its luminescence mechanism. *RSC Adv.* **2017**, *7*, 54002–54007. [[CrossRef](#)]



© 2018 by the authors. Licensee MDPI, Basel, Switzerland. This article is an open access article distributed under the terms and conditions of the Creative Commons Attribution (CC BY) license (<http://creativecommons.org/licenses/by/4.0/>).